ACS APPLIED MATERIALS & INTERFACES

Research Article

www.acsami.org

Electrospun Polyamide 6/Poly(allylamine hydrochloride) Nanofibers Functionalized with Carbon Nanotubes for Electrochemical Detection of Dopamine

Luiza A. Mercante,*[,†] Adriana Pavinatto,[†] Leonardo E. O. Iwaki,[‡] Vanessa P. Scagion,[†,§] Valtencir Zucolotto,[‡] Osvaldo N. Oliveira, Jr.,[‡] Luiz H. C. Mattoso,[†] and Daniel S. Correa*[,†,§]

[†]National Laboratory for Nanotechnology in Agribusiness (LNNA), Embrapa Instrumentation, 13560-970 São Carlos, São Paulo, Brazil

[‡]São Carlos Institute of Physics (IFSC), University of São Paulo (USP), P.O. Box 369, 13566-590 São Carlos, São Paulo, Brazil

[§]Center for Exact Sciences and Technology, Federal University of São Carlos (UFSCar), 13565-905 São Carlos, São Paulo, Brazil

Supporting Information

ABSTRACT: The use of nanomaterials as an electroactive medium has improved the performance of bio/chemical sensors, particularly when synergy is reached upon combining distinct materials. In this paper, we report on a novel architecture comprising electrospun polyamide 6/poly(allylamine hydrochloride) (PA6/PAH) nanofibers functionalized with multiwalled carbon nanotubes, used to detect the neurotransmitter dopamine (DA). Miscibility of PA6 and PAH was sufficient to form a single phase material, as indicated by thermogravimetric analysis (TGA) and differential scanning calorimetry (DSC), leading to nanofibers with no beads onto which the nanotubes could adsorb strongly. Differential pulse voltammetry was employed with indium tin oxide (ITO) electrodes coated with the functionalized nanofibers for the selective electrochemical detection of dopamine (DA), with no interference from uric acid (UA) and ascorbic acid (AA) that are normally present in biological fluids. The response was linear for a DA concentration range from 1 to 70 μmol L^{-1}, with detection limit of 0.15 μmol L^{-1} (S/N = 3). The concepts behind the novel architecture to modify electrodes can be potentially harnessed in other electrochemical sensors and biosensors.

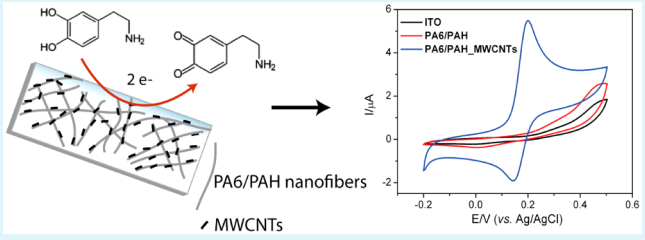

KEYWORDS: *electrospinning, nanofibers, carbon nanotube, dopamine, sensor*

1. INTRODUCTION

Dopamine (DA) is an important neurotransmitter of the catecholamine family with strong influence on the central nervous, renal, cardiovascular and hormonal systems.[1] Abnormal levels of DA have been correlated with various diseases, including Schizophrenia and Parkinson's disease, among others.[2] Therefore, accurate methods to detect DA in biological fluids are crucial to trace and diagnose diseases.[3] Such analytical methods should preferably be cheap and simple to use, which has sparked research into electrochemical sensing, for it can provide rapid response, low cost, simple operation, high sensivity and good selectivity.[4,5] Another stringent requirement for detecting DA efficiently is to avoid interference from uric acid (UA) and ascorbic acid (AA), whose oxidation potentials are close to that of DA. To meet such requirements, modified electrodes can be employed by exploiting nanomaterials.

In this paper, we add to the library of possible materials for DA electrochemical detection by combining electrospun nanofibers and carbon nanotubes. As we shall show, synergy is achieved with this combination. Electrospinning is a versatile, cost-effective method for producing nanofibers in 3D structures with large surface area and high porosity,[6,7] which can be used for sensing.[8−10] In this case, such nanofibers can be modified, for example, with conducting polymers,[11,12] metal oxides nanoparticles,[13] metal nanoparticles[14] and carbon nanostructures[15] as the carbon nanotubes (CNTs). CNTs are interesting for their large surface-to-volume ratio and ability to promote electron transfer reactions.[16,17] Our approach is an alternative to recent nonenzymatic dopamine electrochemical sensors based on electrospun nanofibers,[13,14,18,19] but with no need of thermally treating the modified electrodes to increase electrical conductivity. Such thermal treatment may affect negatively the fibrous morphology of the nanofibers and consequently the sensing ability.[20] Here, the electrospun nanofibers were obtained with polyamide 6 and poly(allylamine hydrochloride) (PAH) and then functionalized with multiwalled carbon nanotubes (MWCNTs). Indium tin oxide (ITO) electrodes coated with these functionalized nanofibers were efficient to

Received: December 10, 2014
Accepted: February 3, 2015
Published: February 3, 2015

DOI: 10.1021/am508709c
ACS Appl. Mater. Interfaces 2015, 7, 4784−4790

detect DA using differential pulse voltammetry (DPV), with no interference from AA and UA.

2. EXPERIMENTAL SECTION

2.1. Materials. Polyamide 6 (PA6, M_w = 20 000 g mol^{-1}), poly(allylamine hydrochloride) (PAH, M_w = 15 000 g mol^{-1}), multiwalled carbon nanotubes functionalized with carboxylic acid (MWCNTs), Triton X-100, dopamine (DA), uric acid (UA) and ascorbic acid (AA) were purchased from Sigma-Aldrich. Formic acid was purchased from Synth Chemical (São Paulo, Brazil). All aqueous solutions were prepared with double-distilled water and the chemicals were used without further purification.

2.2. Electrospinning of PA6 and PA6/PAH Nanofibers. PA6 and PA6/PAH solutions were prepared by dissolving the polymers in formic acid and stirred for 5 h at room temperature. PA6 solution was prepared in concentrations of 20% (w/v), whereas the PA6/PAH solution had 20% (w/v) PA6 and 30% (w/w) PAH. The electrospun nanofibers were obtained by using an electrospinning apparatus at a feed rate of 0.01 mL h^{-1} and an electric voltage of 25 kV. A working distance of 10 cm was kept between the syringe and the metallic collector. The inner diameter of the steel needle was 0.7 mm. Nanofibers were directly electrospun onto indium tin oxide (ITO) glass substrates to obtain modified electrodes. The substrates were attached at the same position in all experiments with an optimal collection time of 10 min. Control of the experimental conditions was important to ensure reproducibility because the diameter and length of nanofibers depend on the collecting time and other parameters associated with electrospinning.

2.3. Adsorption of MWCNTs onto the Electrospun Nanofibers. MWCNTs (0.5 mg mL^{-1}) were dispersed in distilled water (pH 5.0) containing 0.3% (w/w) of surfactant Triton X-100. Ultrasonication at 20 kHz for 2 h was then applied for the dispersion of MWCNT. The electrospun nanofibers deposited on ITO were immersed into the MWCNT solution, rinsed with distilled water and dried under ambient conditions. Various adsorption times for MWCNTs were tested (1, 6, 12 and 24 h) to determine the best dopamine electrochemical response and the time period of 24 h was chosen for subsequent studies (see Figure S1 in the Supporting Information).

2.4. Characterization and Electrochemical Measurements. The morphology of the fibers was evaluated using scanning electron microscopy (SEM, JEOL 6510) operating at 10 kV, with the fiber diameter being estimated with an image analysis software (ImageJ, National Institutes of Health, USA). In each experiment, the average fiber diameter and distribution were determined by measuring 100 random fibers using representative micrographs. For MWCNT-surface modified fibers, morphology was investigated using field-emission gun scanning electron microscopy (FEG-SEM, JEOL-JSM 6701F). Thermogravimetric analysis (TGA) experiments were performed on a thermogravimetric analyzer (Q500 TA Instruments) under nitrogen atmosphere, at a flow rate of 20 mL min^{-1}. Samples in platinum pans were scanned from room temperature to 600 °C at a heating rate of 10 °C min^{-1}. Differential scanning calorimetry (DSC) studies were performed on a calorimetric analyzer (Q100 TA Instruments) under nitrogen atmosphere, at a flow rate of 20 mL min^{-1}. The samples were heated in aluminum pans from −80 to +250 °C at a heating rate of 10 °C min^{-1}.

The electrochemical experiments were performed using a PGSTAT30 Autolab electrochemical system (Metrohm) controlled with GPES software. The ITO-PA6/PAH_MWCNTs electrodes were used as working electrodes. A Pt foil and Ag/AgCl (3 mol L^{-1} KCl) served as the counter (CE) and reference (RE) electrodes, respectively. The experiments were conducted in a 0.01 mol L^{-1} phosphate buffer solution (pH 7.0) at room temperature. The electrochemical measurements were carried out via cyclic voltammetry (CV), differential pulse voltammetry (DPV) and electrochemical impedance spectroscopy (EIS). The CV measurements were performed over a potential range from 0.2 to 0.6 V at a scan rate of 50 mV s^{-1}. The DPV measurements were carried out from 0.2 to 0.6 V with a pulse amplitude of 50 mV, pulse width 0.4 s and pulse period of 0.5 s. EIS measurements were carried out in a 0.05 mol L^{-1} $[Fe(CN)_6]^{3-/4-}$ containing 0.1 mol L^{-1} KCl at a potential of 0.2 V over the frequency range from 0.1 Hz to 100 kHz, using an amplitude of 10 mV.

3. RESULTS AND DISCUSSION

3.1. Characterization of Electrospun Nanofibers. Nanofibers with smooth surfaces without beads are required to decrease the variability of morphology and thus warrant reproducibility.[21,22] The SEM image in Figure 1a indicates that

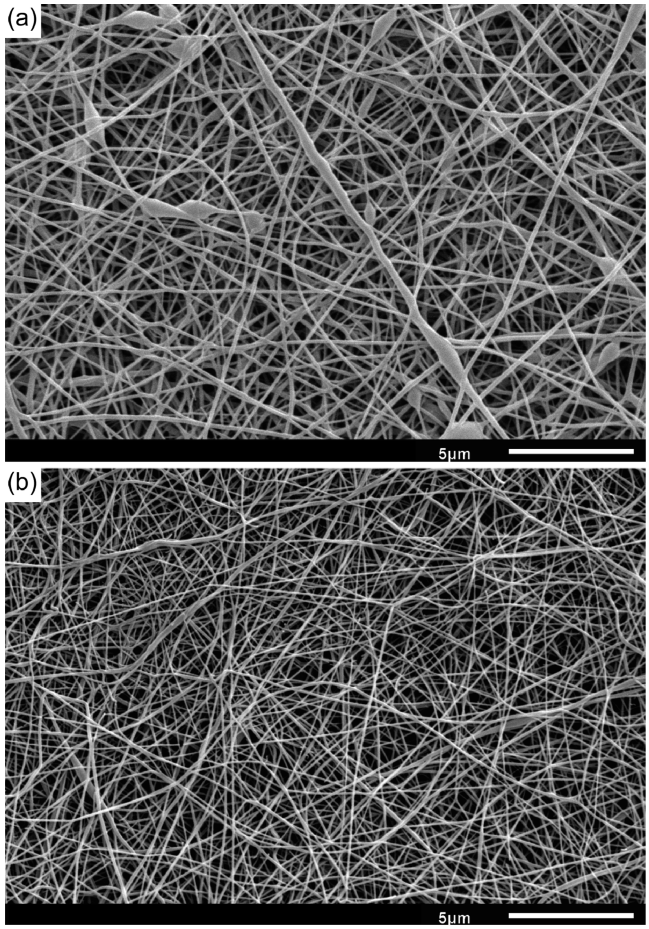

Figure 1. SEM images of (a) PA6 and (b) PA6/PAH nanofibers.

PA6 electrospun fibers contained a few beads along the fiber direction, whose average diameter was 226 ± 82 nm. Therefore, even under optimized conditions there is bead formation, which is a common defect for electrospun nanofibers that impair their use. Incorporation of 30% (w/w) PAH yielded bead-free PA6/PAH fibers with smooth, regular surface morphology, as shown in Figure 1b. The nanofiber diameter also decreased sharply (88 ± 24 nm) because addition of PAH increased the charge density in the solution, leading to smaller and smoother electrospun fibers.[23] These smaller diameters allow for higher contents of active materials, e.g., MWCNTs used here, to adsorb onto the fiber surface.

Miscibility of PA6 and PAH appears to be efficient with formation of a single phase material, as shown by TGA and DSC thermograms in Figure S2 in the Supporting Information. Only one single thermal event was inferred for both TGA and DSC, and the incorporation of PAH in the blend induced a

DOI: 10.1021/am508709c
ACS Appl. Mater. Interfaces 2015, 7, 4784−4790

slight decrease in thermal stability. In the TGA thermogram the maximum weight loss owing to complete decomposition occurred at 440 °C for the blend, to be compared with 450 °C for PA6.[24] Likewise, the melting temperature (T_m) taken from the DSC curves decreased from 215 °C for PA6 to 204 °C for the PA6/PAH nanofibers. The PA6/PAH nanofibers could be efficiently covered with functionalized MWCNTs, as confirmed with the FEG-SEM images in Figure 2. Adsorption

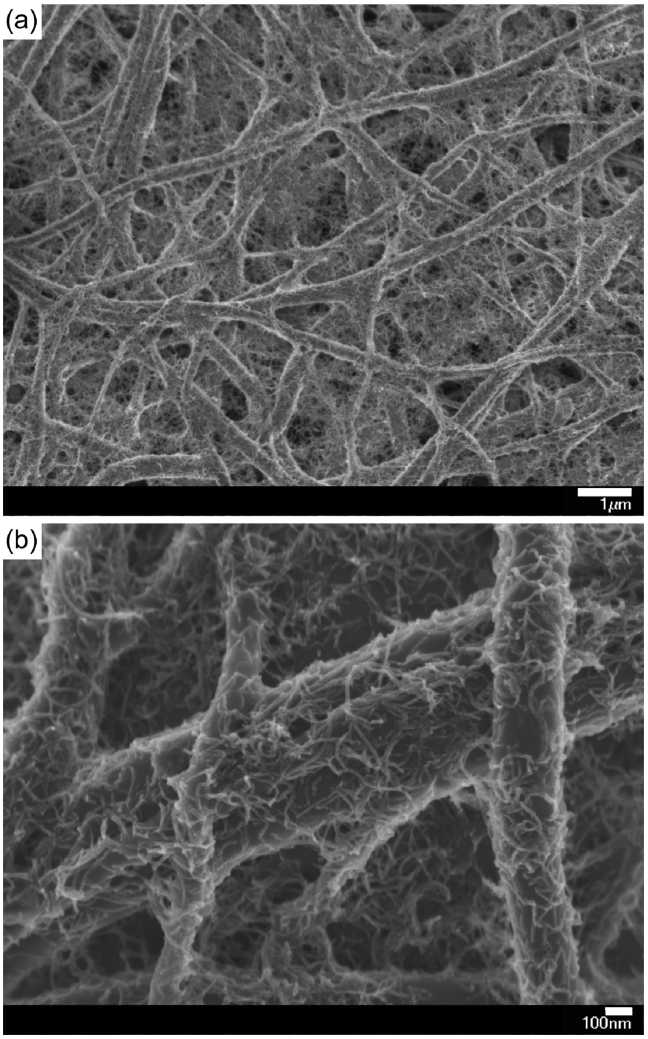

Figure 2. (a) FEG-SEM image of PA6/PAH_MWCNTs nanofibers and (b) magnified image of panel a.

was strong since MWCNTs remained on the surface even after washing. This implies that the MWCNTs are not simply lying on the nanofiber surface. Instead, they are strongly attached to the PA6/PAH nanofibers via H-bonding and/or electrostatic interactions. H-bonding is expected between amide groups (−NHCO−) from PA6 or amine groups (−NH) from PAH and the carboxylic groups (−COOH) from the functionalized MWCNTs.[25,26] As for electrostatic interactions, PAH is fully positively charged at pH 5, because its pK_a is 8.7,[27] and can interact with the partially negatively charged MWCNTs.

3.2. Electrochemical characterization of modified electrodes. The cyclic voltammograms in Figure 3a show a quasi-reversible one-electron redox behavior for all the electrodes in $[Fe(CN)_6]^{3-/4-}$ solution, with peak separation ($\Delta E_p = E_{pa} - E_{pc}$, where E_{pa} and E_{pc} are the anodic and

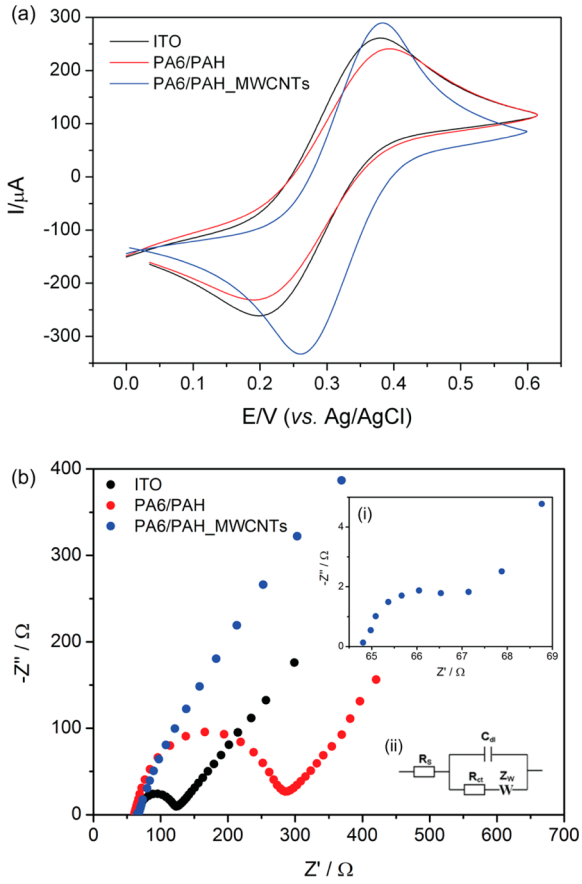

Figure 3. (a) Cyclic voltammograms and (b) Nyquist plots of EIS of ITO, PA6/PAH and PA6/PAH_MWCNTs in a 5 mmol L^{-1} $[Fe(CN)_6]^{3-/4-}$ solution with 0.1 mol L^{-1} KCl. The insets in panel b are related to (i) the close view of PA6/PAH_MWCNTs curve and (ii) the Randle's equivalent circuit model for the impedance data.

cathodic peak potentials, respectively) of 176 mV for ITO, 191 mV for PA6/PAH and 122 mV for PA6/PAH_MWCNTs. Adsorption of PA6/PAH nanofibers caused electrode passivation, as expected, with the anodic peak current (I_{pa}) decreasing from 193 to 177 μA. In contrast, when the ITO electrode was coated with PA6/PAH_MWCNTs, the anodic peak current (I_{pa}) increased to 262 μA. Furthermore, I_{pc} is even higher for PA6/PAH_MWCNTs (247 μA) than for ITO (202 μA). The highest I_{pc} and smallest ΔE_p indicate that PA6/PAH_MWCNTs presents faster electron transfer kinetics between the redox probe solution and the electrode surface when compared with bare ITO and ITO modified with PA6/PAH nanofibers.[13,14,28]

This efficient electron transfer was confirmed in the Nyquist plots in Figure 3b, whose data were analyzed using a Randle's equivalent circuit,[29] shown in the inset. R_s is the electrolyte resistance, C is the interface capacitance, R_{ct} is the charge (electron) transfer resistance and Z_w is the Warburg impedance. The semicircular region at high frequencies is related to an interfacial charge-transfer process and its diameter corresponds to the charge transfer resistance (R_{ct}), whereas the linear region at low frequencies is related to diffusion processes.[30,31] R_{ct} was largest for the PA6/PAH modified electrode (214 Ω) because the nanofibers hinder charge transfer to the ITO interface. For the electrode coated with PA6/PAH_MWCNTs, R_{ct} was only 3 Ω, even lower than that for bare ITO (55 Ω). The result from EIS is consistent with the increased peak current [Fe-

DOI: 10.1021/am508709c
ACS Appl. Mater. Interfaces 2015, 7, 4784−4790

$(CN)_6]^{3-/4-}$ for the PA6/PAH_MWCNTs electrode and a ΔE_p that is even smaller than that for the ITO electrode, as indicated in Figure 3a. The nanofibers provide good dispersion for MWCNTs, thus leading to a large surface area for the electrode and facilitating charge (electron) transfer compared to bare (ITO) and PA6/PAH modified electrodes.[32,33]

3.3. Electrochemical Detection of DA. The favorable electrochemical properties of the electrode coated with PA6/PAH_MWCNTs point to a possible use in a sensor, which is proven here for detection of dopamine (DA). Figure 4 shows a

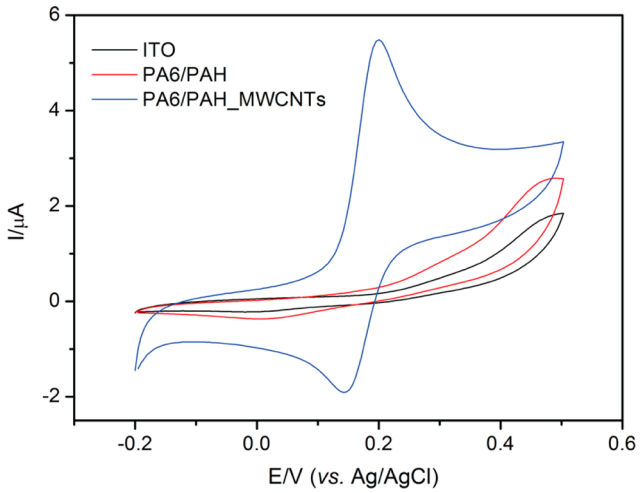

Figure 4. CV curves of 0.05 mmol L^{-1} DA on the surfaces of ITO, PA6/PAH and PA6/PAH_MWCNTs in 0.01 mol L^{-1} PBS solutions (pH 7.0). Scan rate: 50 mV s^{-1}.

prominent redox pair for cyclic voltammogram of the PA6/PAH_MWCNTs electrode in 0.05 mmol L^{-1} DA in a phosphate buffer solution (pH 7.0). No such peaks appear for the ITO and PA6/PAH electrodes, indicating that the electrochemical reaction only occurs at the electroactive MWCNTs sites. The dopamine electrochemical behavior has been proposed to occur via the electron transfer-chemical reaction-electron transfer (ECE) mechanism, which consists in a sequence of electrochemical (E) and chemical (C) reactions, as shown in Scheme 1S (Supporting Information).[34−36] The first step involves DA oxidation to dopaminequinone (DAQ), which reacts chemically generating leucodopaminechrome (LDAC). The latter is then oxidized to dopaminechrome (DAC). Therefore, a pair of redox peaks should be observed at pH = 7.0,[34] and indeed Figure 4 shows two well-defined peaks owing to dopamine detection using the PA6/PAH_MWCNTs electrode. The anodic and cathodic peaks are centered at 0.22 and 0.15 V, respectively, with I_{pa} = 5.5 μA and I_{pc} = 1.4 μA, while ΔE_p was 59 mV. They are assigned to oxidation of DA to DAQ (anodic peak) and reduction of DAQ back to DA (cathodic peak).[35] I_{pc} is much smaller than Ipa, which indicates that these dopamine electrochemical reactions are irreversible at this electrode. The electrochemical process at the PA6/PAH_MWCNTs interface is diffusion controlled, as demonstrated in subsidiary experiments in which the scan rate was varied from 20 mV s^{-1} to 300 mV s^{-1}. Figure S3 in the Supporting Information shows that both cathodic and anodic peak currents increased linearly with the square root of the scan rate.

To verify whether the PA6/PAH_MWCNTs electrode was as efficient in detecting DA as similar sensors, we employed differential pulse voltammetry (DPV), which is advantageous for reaching higher sensitivity by eliminating the non-Faradaic currents that occur in cyclic voltammetry.[30] The DPV curves in Figure 5 show increasing oxidation peak current at approx-

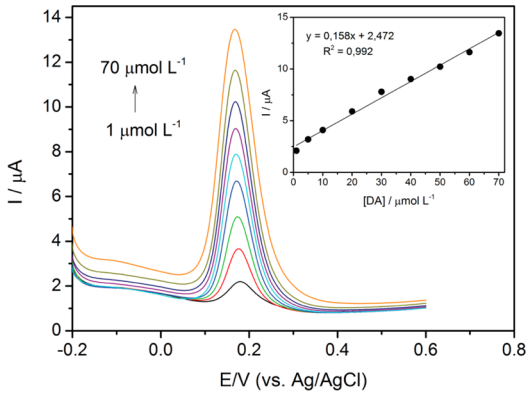

Figure 5. DPV curves for different concentrations of DA (1, 5, 10, 20, 30, 40, 50, 60 and 70 μmol L^{-1}) on PA6/PAH_MWCNTs in 0.01 mol L^{-1} PBS (pH 7.0). Inset: linear relationship between the peak current and DA concentrations.

imately 174 mV with DA concentration. The anodic peak arises from conversion of DA to dopamine-o-quinone,[15] with the current increasing linearly with DA concentration in the range from 1 to 70 μmol L^{-1}, as displayed in the inset. The linear regression equation is I (μA) = 0.158[DA] (μmol L^{-1}) + 2.472 (R^2 = 0.992). The limit of detection reached, 0.15 μmol L^{-1} (S/N = 3), is similar or even better than some recent results reported in the literature, which are listed in Table 1. Therefore, the nanofibers functionalized with carbon nanotubes (PA6/PAH_MWCNTs) are a suitable platform for DA electrochemical detection.

Two potential interfering molecules for dopamine in biological environments are ascorbic acid (AA) and uric acid (UA). We verified that DA can be detected in the presence of AA and UA by performing two types of experiment. In the first, depicted in Figure 6a, we noted that AA gives a negligible signal even when the concentration used (0.1 mmol L^{-1}) was higher than that typically found in human serum (0.08 mmol L^{-1} level).[43] If AA is added simultaneously with UA to a DA-containing sample, again no signal arises from AA, while separate peaks were observed for DA and UA. The second experiment varied DA concentrations for a fixed UA concentration, and again full separation of the corresponding peaks was possible, as indicated in Figure 6b.

We tested the reproducibility of the PA6/PAH_MWCNTs electrode by performing repeated voltammetric experiments with solutions containing 50 μM DA. For ten successive measurements, the relative standard deviation (RSD) was 2.3% for a given electrode, while it increased to 6.6% when three nominally identical electrodes were used. These low RSDs confirm the electrode reproducibility. In addition, electrode stability was studied by measuring the CV curves for 0.05 mmol L^{-1} DA in PBS during 100 cycles at a scan rate of 50 mV s^{-1}. Figure 7 shows that the current assigned to DA oxidation is 82% of the initial value after 100 cycles, thus suggesting good electrode stability owing to an efficient adsorption of MWCNTs on the PA6/PAH nanofibers.

DOI: 10.1021/am508709c
ACS Appl. Mater. Interfaces 2015, 7, 4784−4790

Table 1. Comparison of Composition, Detection Limit and Linear Range of Different Modified Electrodes for Determination of DA

electrode type	modification	detection limit (μmol L^{-1})	linear range (μmol L^{-1})	refs
GCE	Ag-Pt/p-CNFs[a]	0.11	10−500	14
GCE	PANI-GO[b]	0.50	2−18	37
GCE	SWCNH[c]	0.06	0.2−3.8	38
GCE	PEDOT/PNMPy[d]/ AuNPs	2.00−3.00	1−100	39
ITO	Nafion/MWCNT	0.20	0.1−10	40
Au	OPPy[e]/MSA[f]/MWCNTs	0.0004	0.001−2.87	41
CPE	MWCNT	1.07	20−50	42
ITO	PA6/PAH_MWCNTs nanofibers	0.15	1−70	this work

[a]Carbon nanofibers. [b]Graphene oxide. [c]Single-walled carbon nanohorn. [d]Poly(*N*-methylpyrrole). [e]Overoxidized polypyrrole. [f]Mercaptosuccinic acid.

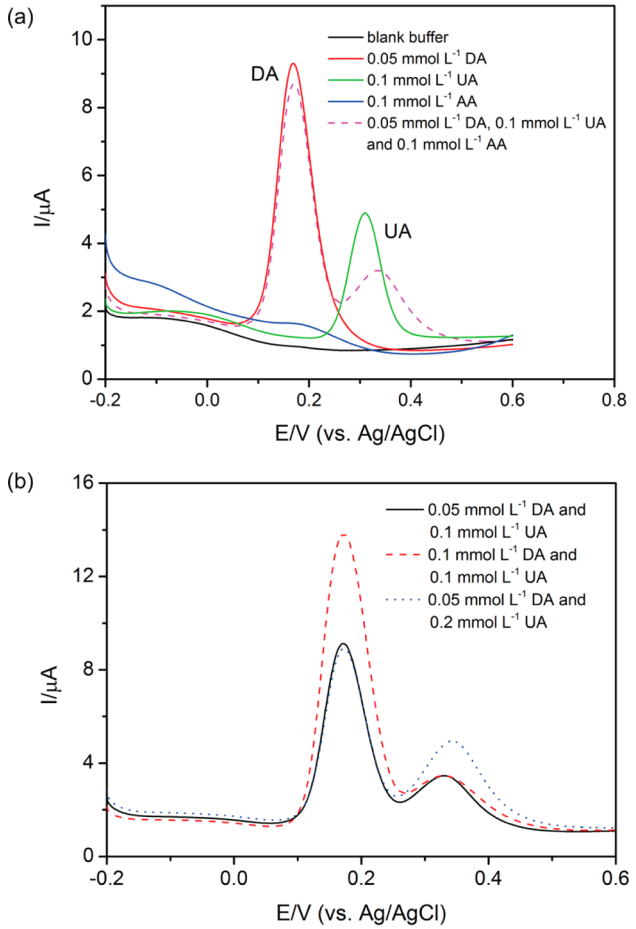

Figure 6. DPV curves for the PA6/PAH_MWCNTs electrode: (a) for detection of DA, AA and UA separately, and then in mixtures with the concentrations indicated in the inset; (b) for simultaneous detection of DA and UA in concentrations ranging from 0.05 to 0.2 mmol L^{-1}.

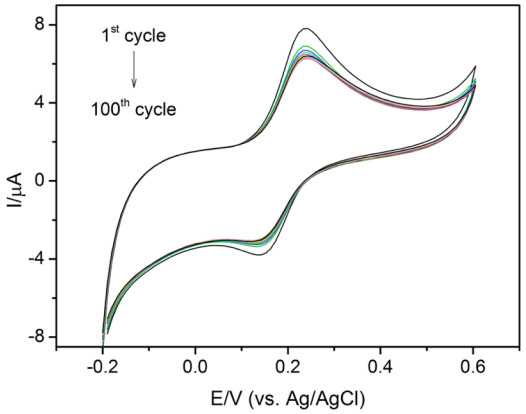

Figure 7. Stability tests for the ITO electrode coated with PA6/PAH_MWCNTs in 0.01 mol L^{-1} (pH 7.0) PBS solution containing 0.05 mmol L^{-1} of DA.

4. CONCLUSION

We fabricated a simple, highly sensitive electrochemical dopamine sensor by functionalizing electrospun polyamide 6/poly(allylamine hydrochloride) (PA6/PAH) nanofibers with multiwalled carbon nanotubes. The as-prepared electrode displayed a good detection limit of 0.15 μmol L^{-1}, high reproducibility and high stability. This sensor may be employed in the selective determination of dopamine in the presence of interfering substances such as ascorbic acid and uric acid. The successful application of this electrode indicates that modified electrospun composite nanofibers provide a new platform for designing sensors to determine dopamine sensitively and selectively.

■ ASSOCIATED CONTENT

Supporting Information

CV curves of 0.05 mmol L^{-1} DA using different MWCNTs adsorption times (Figure S1), TGA and DSC curves (Figure S2), ECE mechanism for dopamine electrochemistry (Scheme 1S) and CV curves of PA6/PAH_MWCNTs in the presence of 0.05 mmol L^{-1} at different scan rates (Figure S3). This material is available free of charge via the Internet at http://pubs.acs.org.

■ AUTHOR INFORMATION

Corresponding Authors

*L. A. Mercante. E-mail: lamercante@gmail.com.
*D. S. Correa. E-mail: daniel.correa@embrapa.br.

Notes

The authors declare no competing financial interest.

■ ACKNOWLEDGMENTS

This work was financially supported by FAPESP (Grant numbers: 2014/16789-5, 2012/23880-3 and 2013/26712-7), CNPq, CAPES, MCTI and EMBRAPA.

■ REFERENCES

(1) Schultz, W. Dopamine Neurons and Their Role in Reward Mechanisms. *Curr. Opin. Neurobiol.* **1997**, *7*, 191−197.

DOI: 10.1021/am508709c
ACS Appl. Mater. Interfaces 2015, 7, 4784−4790

(2) Wightman, R. M.; May, L. J.; Michael, A. C. Detection of Dopamine Dynamics in the Brain. *Anal. Chem.* **1988**, *60*, A769−A779.
(3) Jackowska, K.; Krysinski, P. New Trends in the Electrochemical Sensing of Dopamine. *Anal. Bioanal. Chem.* **2013**, *405*, 3753−3771.
(4) Xue, C.; Han, Q.; Wang, Y.; Wu, J. H.; Wen, T. T.; Wang, R. Y.; Hong, J. L.; Zhou, X. M.; Jiang, H. J. Amperometric Detection of Dopamine in human serum by electrochemical Sensor Based on Gold Nanoparticles Doped Molecularly Imprinted Polymers. *Biosens. Bioelectron.* **2013**, *49*, 199−203.
(5) Ballesteros, C. A. S.; Cancino, J.; Marangoni, V. S.; Zucolotto, V. Nanostructured Fe_3O_4 Satellite Gold Nanoparticles to Improve Biomolecular Detection. *Sens. Actuators, B* **2014**, *198*, 377−383.
(6) Greiner, A.; Wendorff, J. H. Electrospinning: A Fascinating Method for the Preparation of Ultrathin Fibers. *Angew. Chem., Int. Ed.* **2007**, *46*, 5670−5703.
(7) Lu, X.; Wang, C.; Wei, Y. One-Dimensional Composite Nanomaterials: Synthesis by Electrospinning and Their Applications. *Small* **2009**, *5*, 2349−2370.
(8) Ding, B.; Wang, M.; Wang, X.; Yu, J.; Sun, G. Electrospun Nanomaterials for Ultrasensitive Sensors. *Mater. Today* **2010**, *13*, 16−27.
(9) Oliveira, J. E.; Scagion, V. P.; Grassi, V.; Correa, D. S.; Mattoso, L. H. C. Modification of Electrospun Nylon Nanofibers Using Layer-by-Layer Films for Application in Flow Injection Electronic Tongue: Detection of Paraoxon Pesticide in Corn Crop. *Sens. Actuators, B* **2012**, *171*, 249−255.
(10) Sahay, R.; Kumar, P. S.; Sridhar, R.; Sundaramurthy, J.; Venugopal, J.; Mhaisalkarc, S. G.; Ramakrishna, S. Electrospun Composite Nanofibers and Their Multifaceted Applications. *J. Mater. Chem.* **2012**, *22*, 12953−12971.
(11) Lowa, K.; Hornera, C. B.; Lib, C.; Icoa, G.; Boszeb, W.; Myungb, N. V.; Nam, J. Composition-Dependent Sensing Mechanism of Electrospun Conductive Polymer Composite Nanofibers. *Sens. Actuators, B* **2015**, *207*, 235−242.
(12) Roque, A. P.; Mercante, L. A.; Scagion, V. P.; Oliveira, J. E.; Mattoso, L. H. C.; De Boni, L.; Mendonca, C. R.; Correa, D. S. Fluorescent PMMA/MEH-PPV Electrospun Nanofibers: Investigation of Morphology, Solvent, and Surfactant Effect. *J. Polym. Sci., Part B: Polym. Phys.* **2014**, *52*, 1388−1394.
(13) Wu, J.; Yin, F. Studies on the Electrocatalytic Oxidation of Dopamine at Phosphotungstic Acid-ZnO Spun Fiber-Modified Electrode. *Sens. Actuators, B* **2013**, *185*, 651−657.
(14) Huang, Y.; Miao, Y.-E.; Ji, S.; Tjiu, W. W.; Liu, T. Electrospun Carbon Nanofibers Decorated with Ag−Pt Bimetallic Nanoparticles for Selective Detection of Dopamine. *ACS Appl. Mater. Interfaces* **2014**, *6*, 12449−12456.
(15) Ekabutr, P.; Sangsanoh, P.; Rattanarat, P.; Monroe, C. W.; Chailapakul, O.; Supaphol, P. Development of a Disposable Electrode Modified with Carbonized, Graphene-loaded Nanofiber for the Detection of Dopamine in Human Serum. *J. Appl. Polym. Sci.* **2014**, *131*, 40858.
(16) Merkoçi, A.; Pumera, M.; Llopis, X.; Pérez, B.; del Valle, M.; Alegret, S. New Materials for Electrochemical Sensing VI: Carbon Nanotubes. *Trends Anal. Chem.* **2005**, *24*, 826−838.
(17) Gao, C.; Guo, Z.; Liu, J.-H.; Huang, X.-J. The New Age of Carbon Nanotubes: An Updated Review of Functionalized Carbon Nanotubes in Electrochemical Sensors. *Nanoscale* **2012**, *4*, 1948−1963.
(18) Tong, Y.; Li, Z.; Lu, X.; Yang, L.; Sun, W.; Nie, G.; Wang, Z.; Wang, C. Electrochemical Determination of Dopamine Based on Electrospun CeO_2/Au Composite Nanofibers. *Electrochim. Acta* **2013**, *95*, 12−17.
(19) Rodthongkuma, N.; Ruechab, N.; Rangkupana, R.; Vachetd, R. W.; Chailapakule, O. Graphene-loaded Nanofiber-modified Electrodes for the Ultrasensitive Determination Of Dopamine. *Anal. Chim. Acta* **2013**, *804*, 84−91.
(20) Ouyang, Z.; Li, J.; Wang, J.; Li, Q.; Ni, T.; Zhang; Wang, H.; Li, Q.; Su, Z.; Wei, G. Fabrication, Characterization and Sensor Application of Electrospun Polyurethane Nanofibers Filled with Carbon Nanotubes and Silver Nanoparticles. *J. Mater. Chem. B* **2013**, *1*, 2415−2424.
(21) Fong, H.; Chun, I.; Reneker, D. Beaded Nanofibers Formed During Electrospinning. *Polymer* **1999**, 4585−4592.
(22) Liu, Y.; He, J. H.; Yu, J. Y.; Zeng, H. M. Controlling Numbers and Sizes of Beads in Electrospun Nanofibers. *Polym. Int.* **2008**, 632−636.
(23) Son, W. K.; Youk, J. H.; Lee, T. S.; Park, W. H. The Effects of Solution Properties and Polyelectrolyte on Electrospinning of Ultrafine Poly(Ethylene Oxide) Fibers. *Polymer* **2004**, *45*, 2959−2966.
(24) Cho, D.; Zhmayev, E.; Joo, Y. L. Structural Studies of Electrospun Nylon 6 Fibers from Solution and Melt. *Polymer* **2011**, *52*, 4600−4609.
(25) Choi, J.; Park, E. J.; Park, D. W.; Shim, S. E. MWCNT−OH Adsorbed Electrospun Nylon 6,6 Nanofibers Chemiresistor and Their Application in Low Molecular Weight Alcohol Vapours Sensing. *Synth. Methods* **2010**, *160*, 2664−2669.
(26) Kim, H. S.; Jin, H.-J.; Myung, S. J.; Kang, M.; Chin, I.-J. Carbon Nanotube-Adsorbed Electrospun Nanofibrous Membranes of Nylon 6. *Macromol. Rapid Commun.* **2006**, *27*, 146−151.
(27) Petrov, A. I.; Antipov, A. A.; Sukhorukov, G. B. Base-Acid Equilibria in Polyelectrolyte Systems: From Weak Polyelectrolytes to Interpolyelectrolyte Complexes and Multilayered Polyelectrolyte Shells. *Macromolecules* **2003**, *36*, 10079−10086.
(28) Gai, P.; Zhang, H.; Zhang, Y.; Liu, W.; Zhu, G.; Zhang, X.; Chen, J. Simultaneous Electrochemical Detection of Ascorbic Acid, Dopamine and Uric Acid Based on Nitrogen Doped Porous Carbon Nanopolyhedra. *J. Mater. Chem. B* **2013**, *1*, 2742−2749.
(29) Wu, Z.; Wang, B.; Cheng, Z.; Yang, X.; Dong, S.; Wang, E. A Facile Approach to Immobilize Protein for Biosensor: Self-Assembled Supported Bilayer Lipid Membranes on Glassy Carbon Electrode. *Biosens. Bioelectron.* **2001**, *16*, 47−52.
(30) Jiang, J.; Du, X. Sensivite Electrochemical Sensors for Simultaneous Determination of Ascorbic Acid, Dopamine, and Uric Acid Based on Au@Pd-Reduced Graphene Oxide Nanocomposites. *Nanoscale* **2014**, *6*, 11303−11309.
(31) Wang, Q.; Moser, J. E.; Gratzel, M. Electrochemical Impedance Spectroscopic Analysis of Dye-Sensitized Solar Cells. *J. Phys. Chem. B* **2005**, *109*, 14945−14953.
(32) Gao, J.; Hu, M.; Li, R. K. Y. Ultrasonication Induced Absorption of Carbon Nanotubes onto Electrospun Nanofibers with Improved Thermal and Electrical Performances. *J. Mater. Chem.* **2012**, *22*, 10867−10872.
(33) Ragupathya, D.; Gopalana, A. I.; Lee, K.-P. Electrocatalytic Oxidation and Determination of Ascorbic Acid in the Presence of Dopamine at Multiwalled Carbon Nanotube−Silica Network−Gold Nanoparticles based Nanohybrid Modified Electrode. *Sens. Actuators, B* **2010**, *143*, 696−703.
(34) Li, Y.; Liu, M.; Xiang, C.; Xie, Q.; Yao, S. Electrochemical Quartz Crystal Microbalance Study on Growth and Property of the Polymer Deposit at Gold Electrodes During Oxidation of Dopamine in Aqueous Solutions. *Thin Solid Films* **2006**, *497*, 270−278.
(35) Hsu, M.-S.; Chen, Y.-L.; Lee, C.-Y.; Chiu, H.-T. Gold Nanostructures on Flexible Substrates as Electrochemical Dopamine Sensors. *ACS Appl. Mater. Interfaces* **2012**, *4*, 5570−5575.
(36) Zhao, J.; Zhang, W.; Sherrell, P.; Razal, J. M.; Huang, X.-F.; Minett, A. I.; Chen, J. Carbon Nanotube Nanoweb-Bioelectrode for Highly Selective Dopamine Sensing. *ACS Appl. Mater. Interfaces* **2012**, *4*, 44−48.
(37) Manivel, P.; Dhakshnamoorthy, M.; Balamurugan, A.; Ponpandian, N.; Mangalaraj, D.; Viswanathan, C. Conducting Polyaniline-graphene Oxide Fibrous Nanocomposites: Preparation, Characterization and Simultaneous Electrochemical Detection of Ascorbic Acid, Dopamine and Uric Acid. *RSC Adv.* **2013**, *3*, 14428−14437.
(38) Zhu, S. Y.; Li, H. J.; Niu, W. X.; Xu, G. B. Simultaneous Electrochemical Determination of Uric Acid, Dopamine, and Ascorbic Acid at Single-Walled Carbon Nanohorn Modified Glassy Carbon Electrode. *Biosens. Bioelectron.* **2009**, *25*, 940−943.

DOI: 10.1021/am508709c
ACS Appl. Mater. Interfaces 2015, 7, 4784−4790

(39) Fabregat, G.; Armelin, E.; Alemán, C. Selective Detection of Dopamine Combining Multilayers of Conducting Polymers with Gold Nanoparticles. *J. Phys. Chem. B* **2014**, *118*, 4669−4682.
(40) Zhao, J.; Yu, Y.; Weng, B.; Zhang, W.; Harris, A. T.; Minett, A. I.; Yue, Z.; Huang, X.-F.; Chen, J. Sensitive and Selective Dopamine Determination in Human Serum With Inkjet Printed Nafion/MWCNT Chips. *Electrochem. Commun.* **2013**, *37*, 32−35.
(41) Su, Z.; Liu, Y.; Xie, Q.; Chen, L.; Zhang, Y.; Meng, Y.; Li, Y.; Fu, Y.; Ma, M.; Yao, S. Preparation of Thiolated Polymeric Nanocomposite for Sensitive Electroanalysis of Dopamine. *Biosens. Bioelectron.* **2012**, *36*, 154−160.
(42) Ghoreishi, S. M.; Behpour, M.; Mousavi, S.; Khoobi, A.; Ghoreishi, F. S. Simultaneous Electrochemical Determination of Dopamine, Ascorbic Acid and Uric Acid in the Presence of Sodium Dodecyl Sulphate Using a Multi-Walled Carbon Nanotube Modified Carbon Paste Electrode. *RSC Adv.* **2014**, *4*, 37979−37984.
(43) Chauhan, N.; Narang, J.; Pundir, C. S. Fabrication of Multiwalled Carbon Nanotubes/Polyaniline Modified Au Electrode for Ascorbic Acid Determination. *Analyst* **2011**, *136*, 1938−1945.

DOI: 10.1021/am508709c
ACS Appl. Mater. Interfaces 2015, 7, 4784−4790